

添付資料3 国際学会発表資料
第36回赤外ミリ波テラヘルツ波国際会議発表資料



UNIVERSITY OF
CAMBRIDGE

TeraView

Time-course analysis of tablet film-coating using terahertz pulsed imaging

Tomoaki Sakamoto^a, Koji Nakayama^b, Alessia Portier^c, Donald Arnone^c, Daisuke Sasakura^d, Philip Taday^c, Axel Zeitler^d, Toru Kawanishi^e, and Yukio Hiyama^a

^a Division of Drugs, National Institute of Health Sciences, Tokyo 158-8501, Japan

^b Towa Pharmaceutical Co., Ltd., Osaka 571-0033, Japan

^c TeraView Ltd., Cambridge CB4 0WS, United Kingdom

^d Malvern Instrument Japan, A Division of Spectris Co.Ltd, Tokyo 101-0048, Japan

^e Department of Chemical Engineering and Biotechnology, University of Cambridge, Cambridge CB2 3RA, United Kingdom

Introduction

A coating has an important role to keep a quality of pharmaceutical such as a masking of bitter taste, a moisture-protecting or light-protecting, and so on. Therefore, it is necessary to control about these coating processes as one of the critical quality factors in a manufacturing process. In order to release a pharmaceutical product which has high quality, confirmation of critical quality profiles on a developing stage and introduction of suitable evaluation methods into a manufacturing process would be necessary. The authors have investigated concerning an applicability of terahertz electro-magnetic wave technology for a quality evaluation method and a process control tool for pharmaceuticals. A terahertz pulsed imaging (TPI) can be used to acquire structural and physical information such as an existence of layers and a change of density by delayed reflectance derived from a change of refractive index of terahertz pulse. The authors will present a tablet-coating quality analysis in a coating process using TPI.

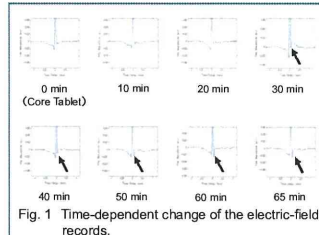


Fig. 1 Time-dependent change of the electric-field records.

Conclusion

➢ Formation of coating layer was started around the embossing at 30 min after the coating process was started.

➢ The negative peak which represents the formation of coat layer was detected on the electric-field records from 30 min.

➢ The intensity of the reflected terahertz pulsed waves was increased with the passage of time.

➢ The coating thickness was correctly calculated after 40 min of the elapsed time.

➢ The variance of the coating thickness after 60 min were getting bigger.

Experimental



Core tablets
API 10 w/w%
Major ingredient(Lactose monohydrate)
Approx. 50w/w%
Other ingredients (total approx. 40 w/w%)

Collection time: 0 min(core tablet), 10 min, 20 min, 30 min, 40 min, 50 min, 60 min, 65 min

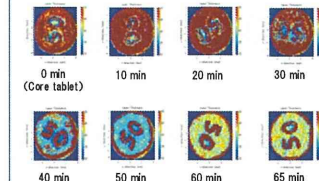


Fig. 2 Time-dependent change of the intensities of reflected terahertz wave.

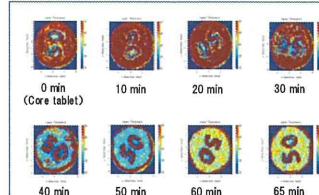


Fig. 3 Time-dependent change of the coating thickness.

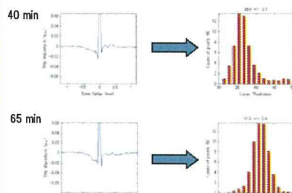


Fig. 5 Electric-field records and histograms of coating thickness of the tablets collected at 40 min and 65 min.

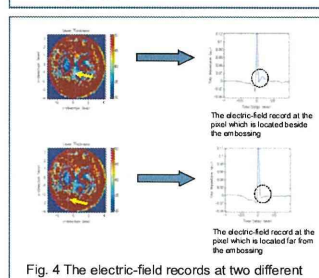


Fig. 4 The electric-field records at two different positions (30 min-tablet).

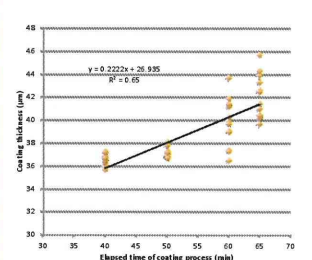


Fig. 6 Correlation between the elapsed time and the coating thickness.



添付資料4 国内学会発表要旨 1

IUPAC International Congress on Analytical Sciences 2011発表要旨

VIBRATIONAL SPECTROSCOPIC ANALYSIS OF PHARMACEUTICALS AND TABLET PROCESSES UNDERSTANDING USING NEAR-, MID-, AND FAR-INFRARED / TERAHERTZ SPECTROSCOPY

Tomoaki Sakamoto,¹ Koji Nakayama,² Daisuke Sasakura,³ Toru Kawanishi,¹ Yukio Hiyama,¹

¹Division of Drugs, National Institute of Health Sciences, Tokyo 158-8501, Japan, ²Towa Pharmaceutical Co., Ltd. Osaka 571-0033, Japan, ³Bruker Optics K.K. Tokyo 110-0016, Japan.

Correspondence: tsakamot@nihs.go.jp

Qualitative attribute based on a vibrational spectroscopic characterization of pharmaceutical granules made by three kinds of production processes (a direct compaction, a share granulation and a fluid-bed granulation) were evaluated using a near-infrared (NIR), a mid-infrared (MIR) and a far-infrared (FIR) /terahertz (THz) spectrometers. For a NIR, a MIR or a FIR/THz measurement, a MPA Fourier-transform NIR spectrometer (Bruker Optik GmbH, Ettlingen, Germany) or a IR-6300 Fourier-transform IR spectrometer (JASCO, Tokyo, Japan) was used. The measurement range, resolution and scan number were set at 12500 cm⁻¹ to 4000 cm⁻¹, 2 cm⁻¹ and 128, for a NIR measurement, 4000 cm⁻¹ to 400 cm⁻¹, 1 cm⁻¹ and 64 for a MIR measurement, and 220 cm⁻¹ to 20 cm⁻¹, 4 cm⁻¹ and 512 for a FIR/THz measurement, respectively. The NIR spectra, the MIR spectra or the FIR/THz spectra were obtained by a diffuse-reflectance mode, an ATR mode or a transmittance-reflectance mode, respectively. The samples that contained theophylline (TP) of 10 w/w% as an active pharmaceutical ingredient (API) were used. In the NIR spectra, the significant difference of spectral features at 4300 cm⁻¹ which was included in C-H combination region was observed. The absorptions derived from TP and lactose monohydrate (LT) were detected at these peak positions. From the MIR spectra of TP and LT and their chemical structure, the absorption at 4303 cm⁻¹ (TP) or 4306 cm⁻¹ (LT) was assigned as a combination of C-H stretching and CH₂ deformation (TP: N-CH₃, LT: CH₂OH). In the ATR-MIR spectra obtained from the mixture of TP and HPC-L under dry condition ([T+H (D)]) or from granules made by a wet granulation([T+H (W)]), an absorption at 1048 cm⁻¹ (C-N stretching of N-CH₃ derived from TP) disappeared in the spectrum obtained from [T+H (W)]. This observation strongly suggests that a C-N stretching is affected by an interaction between TP and HPC-L under a wet granulation process. The two major absorptions of TP in the FIR/THz spectrum obtained from [T+H (W)] also disappeared, though these absorptions were observed in the spectrum obtained from [T+H (D)]. The absorption at 1700 cm⁻¹ (C=O stretching) also disappeared on the spectrum obtained from [T+H (W)]. This observation suggests that a functional group "C=O" in TP would be mainly interacted to HPC-L under a wet condition. The authors predict that the interaction of C=O affects C-H combination derived from an adjacent functional group "N-CH₃". A vibrational analysis using an electro-magnetic wave in an infra-red region would contribute not only for understanding of quality attribute of a pharmaceutical process but also for obtaining basic spectroscopic information which is useful for efficient quality control of pharmaceutical products.

添付資料5 国内学会発表資料1

IUPAC International Congress on Analytical Sciences 2011ポスター発表資料



VIBRATIONAL SPECTROSCOPIC ANALYSIS OF PHARMACEUTICALS AND TABLET PROCESSES UNDERSTANDING USING NEAR-, MID-, AND FAR-INFRARED / TERAHERTZ SPECTROSCOPY

Tomoaki Sakamoto,¹ Koji Nakayama,² Daisuke Sasakura,³ Toru Kawanishi,¹ Yukio Hiyama,¹

¹Division of Drugs, National Institute of Health Sciences, Tokyo 158-8501, Japan, ²Towa Pharmaceutical Co., Ltd. Osaka 571-0033, Japan, ³Bruker Optics K.K. Tokyo 110-0016, Japan. Correspondence: tsakamot@nihs.go.jp

Introduction

In order to achieve an effective links between the concepts of ICH Q series and practical manufacturing quality control, it is important to have technologies that can scrutinize a quality attribute of a pharmaceutical product through a life cycle if it is very important. Especially, to analyze quality attributes would contribute to the quality of quality attributes such as Quality by Design (QbD). In this study, we focused on quality differences of ingredients in pharmaceutical granules and tablet manufacturing processes. The characteristic qualities on vibrational spectroscopic characterization of pharmaceutical granules made by three kinds of production process (a direct compression, a slugging and granulation, and bed granulation) were evaluated using a near-infrared (NIR), a mid-infrared (MIR) and a far-infrared (FIR)/terahertz (THz) spectrometers.

Results

| Instruments and Analytical Condition | |
|--------------------------------------|--|
| Instrument | Bruker FT-NIR Spectrometer (Bruker Optics) |
| Measurement range | 12000-4000 cm ⁻¹ |
| Resolution | 2 cm ⁻¹ |
| Scan numbers | 128 |

Fig. 1 Near-IR spectra obtained from MP for DC (blue solid line), Gra by SG (red solid line), Gra by FG (green solid line), TP (the orange broken line), and LT (the purple broken line).

(A) Off-line spectra, (B) Second derivative spectra.

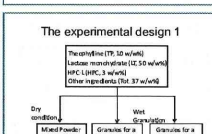


Fig. 2 NIR spectra of MP for DC (blue solid line), Gra by SG (red solid line), and Gra by FG (green solid line).

(A) Off-line spectra, (B) Second derivative spectra.

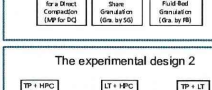


Fig. 3 ATR IR spectra of MP for DC (blue solid line), Gra by SG (red solid line), and Gra by FG (green solid line).

(A) Off-line spectra, (B) Second derivative spectra.



Fig. 4 Chemical structures of two main ingredients used in this study

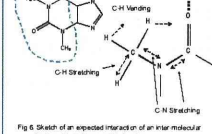
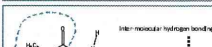


Fig. 6 Sketch of an expected interaction of an inter-molecular hydrogen bonding on amide function

Fig. 7 ATR-MIR spectra of a stretching of carbonyl C=O obtained from (TP+H) (D) (the blue solid line), (TP+H) (W) (the blue solid line), TP (the orange broken line), HPC-L (the green broken line).

(A) Off-line spectra, (B) Second derivative spectra.

The absorbance of the amide II disappear on the spectrum of (TP+H) (W).

Fig. 8 ATR-MIR spectra of a stretching of carbonyl C=O obtained from (TP+H) (D) (the blue solid line), (TP+H) (W) (the blue solid line), TP (the orange broken line), and LT (the purple broken line).

(A) Off-line spectra, (B) Second derivative spectra.

The absorbance of the amide II disappear on the spectrum of (TP+H) (W).

Fig. 9 ATR-MIR spectra of a stretching of carbonyl C=O obtained from (TP+H) (D) (the blue solid line), (TP+H) (W) (the blue solid line), TP (the orange broken line), and LT (the purple broken line).

(A) Off-line spectra, (B) Second derivative spectra.

The absorbance of the amide II disappear on the spectrum of (TP+H) (W).

Fig. 10 ATR-MIR spectra of O-H stretching obtained from (TP+H) (D) (the blue solid line), TP (the orange broken line), TP (the orange broken line), and LT (the purple broken line).

The peak at 1200 cm⁻¹ derived from LT in the spectrum of (TP+H) (W) significantly decreased compared with that of (TP+H) (D).

Fig. 11 Offset FIR/THz spectra obtained from MP for DC (DC (the red solid line), Gra by SG (the green solid line), Gra by FG (the orange broken line), TP (the purple broken line)).

The two characteristic absorptions disappeared due to a low amount of TP.

Fig. 12 Offset FIR/THz spectra obtained from (TP+H) (D) (the red solid line), (TP+H) (W) (the blue solid line), TP (the orange broken line), and LT (the purple broken line).

The peak positions of O-H combination on the spectra obtained from (TP+H) (D) and (W) are same.

The absorbance of the amide II disappear on the spectrum of (TP+H) (W).

Fig. 13 Offset FIR/THz spectra obtained from (TP+H) (D) (the red solid line), (TP+H) (W) (the blue solid line), TP (the orange broken line), and HPC (the light green broken line).

The two characteristic absorptions disappear on the spectrum of (TP+H) (W).

Conclusions

> Differences of the waveforms on C-H combination derived from -NH₂ of theophylline and -CH₂OH of lactose monohydrate were observed in the three different tablet manufacturing processes.

> Differences of the absorption at C-H combination obtained from granules of theophylline and lactose were observed.

> Using ATR-MIR spectra analysis of granules using ATR-MIR indicates the tertiary amide of theophylline is contributed to an interaction such as an inter-molecular hydrogen bonding with HPC (C-N stretching and C=O stretching).

> No spectroscopic difference on C-H combination region was observed from the granules made from lactose and HPC.

> According to ATR-MIR spectroscopic observation of granules made from theophylline and lactose, C-H bending (-CH₂OH) of lactose was observed by a sharp peak. However, no interaction such as an inter-molecular hydrogen bonding occurred between both compounds. (No differences of the waveforms on O-H combination and C=O stretching were observed.)

> Although the characteristic absorptions on FIR/THz region obtained from the mixture of theophylline - HPC or lactose - HPC were observed in dry condition, those absorptions disappeared on the spectra of the granules. These observation may be caused by formation of an inter-molecular interaction or by change of a crystal structure of the actives.

> It was suggested that theophylline absorptions were generated by different cyclization mechanisms during a wet granulation process.

> Vibrational spectroscopic analysis using an electro-magnetic wave in infra-red region (near-infrared, mid-infrared and far-infrared/THz) would provide useful information to scrutinize quality attribute such as molecular vibration of a pharmaceutical product in a process.

Fig. 14 Off-line FIR/THz spectra of the O-H bending region obtained from (TP+H) (D) (the red solid line), TP (the orange broken line), and LT (the purple broken line).

(A) Off-line spectra, (B) Second derivative spectra.

The peak at 3400 cm⁻¹ derived from LT in the spectrum of (TP+H) (W) disappears.

Fig. 15 Off-line FIR/THz spectra obtained from (TP+H) (D) (the red solid line), (TP+H) (W) (the blue solid line), TP (the orange broken line), and LT (the purple broken line).

The two characteristic absorptions disappear on the spectrum of (TP+H) (W).

Fig. 16 Off-line FIR/THz spectra obtained from (TP+H) (D) (the red solid line), (TP+H) (W) (the blue solid line), TP (the orange broken line), and HPC (the light green broken line).

The two characteristic absorptions disappear on the spectrum of (TP+H) (W).

Fig. 17 Off-line FIR/THz spectra obtained from (TP+H) (D) (the red solid line), (TP+H) (W) (the blue solid line), TP (the orange broken line), and LT (the purple broken line).

The peak positions of O-H combination on the spectra obtained from (TP+H) (D) and (W) are same.

The absorbance of the amide II disappear on the spectrum of (TP+H) (W).

Fig. 18 Off-line FIR/THz spectra obtained from (TP+H) (D) (the red solid line), (TP+H) (W) (the blue solid line), TP (the orange broken line), and LT (the purple broken line).

The peak positions of O-H combination on the spectra obtained from (TP+H) (D) and (W) are same.

The absorbance of the amide II disappear on the spectrum of (TP+H) (W).

Fig. 19 Off-line FIR/THz spectra obtained from (TP+H) (D) (the red solid line), (TP+H) (W) (the blue solid line), TP (the orange broken line), and HPC (the light green broken line).

The two characteristic absorptions disappear on the spectrum of (TP+H) (W).

Fig. 20 Off-line FIR/THz spectra obtained from (TP+H) (D) (the red solid line), (TP+H) (W) (the blue solid line), TP (the orange broken line), and LT (the purple broken line).

The peak positions of O-H combination on the spectra obtained from (TP+H) (D) and (W) are same.

The absorbance of the amide II disappear on the spectrum of (TP+H) (W).

Fig. 21 Off-line FIR/THz spectra obtained from (TP+H) (D) (the red solid line), (TP+H) (W) (the blue solid line), TP (the orange broken line), and LT (the purple broken line).

The peak positions of O-H combination on the spectra obtained from (TP+H) (D) and (W) are same.

The absorbance of the amide II disappear on the spectrum of (TP+H) (W).

Fig. 22 Off-line FIR/THz spectra obtained from (TP+H) (D) (the red solid line), (TP+H) (W) (the blue solid line), TP (the orange broken line), and HPC (the light green broken line).

The two characteristic absorptions disappear on the spectrum of (TP+H) (W).

Fig. 23 Off-line FIR/THz spectra obtained from (TP+H) (D) (the red solid line), (TP+H) (W) (the blue solid line), TP (the orange broken line), and LT (the purple broken line).

The peak positions of O-H combination on the spectra obtained from (TP+H) (D) and (W) are same.

The absorbance of the amide II disappear on the spectrum of (TP+H) (W).

Fig. 24 Off-line FIR/THz spectra obtained from (TP+H) (D) (the red solid line), (TP+H) (W) (the blue solid line), TP (the orange broken line), and LT (the purple broken line).

The peak positions of O-H combination on the spectra obtained from (TP+H) (D) and (W) are same.

The absorbance of the amide II disappear on the spectrum of (TP+H) (W).

Fig. 25 Off-line FIR/THz spectra obtained from (TP+H) (D) (the red solid line), (TP+H) (W) (the blue solid line), TP (the orange broken line), and HPC (the light green broken line).

The two characteristic absorptions disappear on the spectrum of (TP+H) (W).

Fig. 26 Off-line FIR/THz spectra obtained from (TP+H) (D) (the red solid line), (TP+H) (W) (the blue solid line), TP (the orange broken line), and LT (the purple broken line).

The peak positions of O-H combination on the spectra obtained from (TP+H) (D) and (W) are same.

The absorbance of the amide II disappear on the spectrum of (TP+H) (W).

Fig. 27 Off-line FIR/THz spectra obtained from (TP+H) (D) (the red solid line), (TP+H) (W) (the blue solid line), TP (the orange broken line), and HPC (the light green broken line).

The two characteristic absorptions disappear on the spectrum of (TP+H) (W).

Fig. 28 Off-line FIR/THz spectra obtained from (TP+H) (D) (the red solid line), (TP+H) (W) (the blue solid line), TP (the orange broken line), and LT (the purple broken line).

The peak positions of O-H combination on the spectra obtained from (TP+H) (D) and (W) are same.

The absorbance of the amide II disappear on the spectrum of (TP+H) (W).

Fig. 29 Off-line FIR/THz spectra obtained from (TP+H) (D) (the red solid line), (TP+H) (W) (the blue solid line), TP (the orange broken line), and HPC (the light green broken line).

The two characteristic absorptions disappear on the spectrum of (TP+H) (W).

Fig. 30 Off-line FIR/THz spectra obtained from (TP+H) (D) (the red solid line), (TP+H) (W) (the blue solid line), TP (the orange broken line), and LT (the purple broken line).

The peak positions of O-H combination on the spectra obtained from (TP+H) (D) and (W) are same.

The absorbance of the amide II disappear on the spectrum of (TP+H) (W).

Fig. 31 Off-line FIR/THz spectra obtained from (TP+H) (D) (the red solid line), (TP+H) (W) (the blue solid line), TP (the orange broken line), and HPC (the light green broken line).

The two characteristic absorptions disappear on the spectrum of (TP+H) (W).

Fig. 32 Off-line FIR/THz spectra obtained from (TP+H) (D) (the red solid line), (TP+H) (W) (the blue solid line), TP (the orange broken line), and LT (the purple broken line).

The peak positions of O-H combination on the spectra obtained from (TP+H) (D) and (W) are same.

The absorbance of the amide II disappear on the spectrum of (TP+H) (W).

Fig. 33 Off-line FIR/THz spectra obtained from (TP+H) (D) (the red solid line), (TP+H) (W) (the blue solid line), TP (the orange broken line), and HPC (the light green broken line).

The two characteristic absorptions disappear on the spectrum of (TP+H) (W).

Fig. 34 Off-line FIR/THz spectra obtained from (TP+H) (D) (the red solid line), (TP+H) (W) (the blue solid line), TP (the orange broken line), and LT (the purple broken line).

The peak positions of O-H combination on the spectra obtained from (TP+H) (D) and (W) are same.

The absorbance of the amide II disappear on the spectrum of (TP+H) (W).

Fig. 35 Off-line FIR/THz spectra obtained from (TP+H) (D) (the red solid line), (TP+H) (W) (the blue solid line), TP (the orange broken line), and HPC (the light green broken line).

The two characteristic absorptions disappear on the spectrum of (TP+H) (W).

Fig. 36 Off-line FIR/THz spectra obtained from (TP+H) (D) (the red solid line), (TP+H) (W) (the blue solid line), TP (the orange broken line), and LT (the purple broken line).

The peak positions of O-H combination on the spectra obtained from (TP+H) (D) and (W) are same.

The absorbance of the amide II disappear on the spectrum of (TP+H) (W).

Fig. 37 Off-line FIR/THz spectra obtained from (TP+H) (D) (the red solid line), (TP+H) (W) (the blue solid line), TP (the orange broken line), and HPC (the light green broken line).

The two characteristic absorptions disappear on the spectrum of (TP+H) (W).

Fig. 38 Off-line FIR/THz spectra obtained from (TP+H) (D) (the red solid line), (TP+H) (W) (the blue solid line), TP (the orange broken line), and LT (the purple broken line).

The peak positions of O-H combination on the spectra obtained from (TP+H) (D) and (W) are same.

The absorbance of the amide II disappear on the spectrum of (TP+H) (W).

Fig. 39 Off-line FIR/THz spectra obtained from (TP+H) (D) (the red solid line), (TP+H) (W) (the blue solid line), TP (the orange broken line), and HPC (the light green broken line).

The two characteristic absorptions disappear on the spectrum of (TP+H) (W).

Fig. 40 Off-line FIR/THz spectra obtained from (TP+H) (D) (the red solid line), (TP+H) (W) (the blue solid line), TP (the orange broken line), and LT (the purple broken line).

The peak positions of O-H combination on the spectra obtained from (TP+H) (D) and (W) are same.

The absorbance of the amide II disappear on the spectrum of (TP+H) (W).

Fig. 41 Off-line FIR/THz spectra obtained from (TP+H) (D) (the red solid line), (TP+H) (W) (the blue solid line), TP (the orange broken line), and HPC (the light green broken line).

The two characteristic absorptions disappear on the spectrum of (TP+H) (W).

Fig. 42 Off-line FIR/THz spectra obtained from (TP+H) (D) (the red solid line), (TP+H) (W) (the blue solid line), TP (the orange broken line), and LT (the purple broken line).

The peak positions of O-H combination on the spectra obtained from (TP+H) (D) and (W) are same.

The absorbance of the amide II disappear on the spectrum of (TP+H) (W).

Fig. 43 Off-line FIR/THz spectra obtained from (TP+H) (D) (the red solid line), (TP+H) (W) (the blue solid line), TP (the orange broken line), and HPC (the light green broken line).

The two characteristic absorptions disappear on the spectrum of (TP+H) (W).

Fig. 44 Off-line FIR/THz spectra obtained from (TP+H) (D) (the red solid line), (TP+H) (W) (the blue solid line), TP (the orange broken line), and LT (the purple broken line).

The peak positions of O-H combination on the spectra obtained from (TP+H) (D) and (W) are same.

The absorbance of the amide II disappear on the spectrum of (TP+H) (W).

Fig. 45 Off-line FIR/THz spectra obtained from (TP+H) (D) (the red solid line), (TP+H) (W) (the blue solid line), TP (the orange broken line), and HPC (the light green broken line).

The two characteristic absorptions disappear on the spectrum of (TP+H) (W).

Fig. 46 Off-line FIR/THz spectra obtained from (TP+H) (D) (the red solid line), (TP+H) (W) (the blue solid line), TP (the orange broken line), and LT (the purple broken line).

The peak positions of O-H combination on the spectra obtained from (TP+H) (D) and (W) are same.

The absorbance of the amide II disappear on the spectrum of (TP+H) (W).

Fig. 47 Off-line FIR/THz spectra obtained from (TP+H) (D) (the red solid line), (TP+H) (W) (the blue solid line), TP (the orange broken line), and HPC (the light green broken line).

The two characteristic absorptions disappear on the spectrum of (TP+H) (W).

Fig. 48 Off-line FIR/THz spectra obtained from (TP+H) (D) (the red solid line), (TP+H) (W) (the blue solid line), TP (the orange broken line), and LT (the purple broken line).

The peak positions of O-H combination on the spectra obtained from (TP+H) (D) and (W) are same.

The absorbance of the amide II disappear on the spectrum of (TP+H) (W).

Fig. 49 Off-line FIR/THz spectra obtained from (TP+H) (D) (the red solid line), (TP+H) (W) (the blue solid line), TP (the orange broken line), and HPC (the light green broken line).

The two characteristic absorptions disappear on the spectrum of (TP+H) (W).

Fig. 50 Off-line FIR/THz spectra obtained from (TP+H) (D) (the red solid line), (TP+H) (W) (the blue solid line), TP (the orange broken line), and LT (the purple broken line).

The peak positions of O-H combination on the spectra obtained from (TP+H) (D) and (W) are same.

The absorbance of the amide II disappear on the spectrum of (TP+H) (W).

Fig. 51 Off-line FIR/THz spectra obtained from (TP+H) (D) (the red solid line), (TP+H) (W) (the blue solid line), TP (the orange broken line), and HPC (the light green broken line).

The two characteristic absorptions disappear on the spectrum of (TP+H) (W).

Fig. 52 Off-line FIR/THz spectra obtained from (TP+H) (D) (the red solid line), (TP+H) (W) (the blue solid line), TP (the orange broken line), and LT (the purple broken line).

The peak positions of O-H combination on the spectra obtained from (TP+H) (D) and (W) are same.

The absorbance of the amide II disappear on the spectrum of (TP+H) (W).

Fig. 53 Off-line FIR/THz spectra obtained from (TP+H) (D) (the red solid line), (TP+H) (W) (the blue solid line), TP (the orange broken line), and HPC (the light green broken line).

The two characteristic absorptions disappear on the spectrum of (TP+H) (W).

Fig. 54 Off-line FIR/THz spectra obtained from (TP+H) (D) (the red solid line), (TP+H) (W) (the blue solid line), TP (the orange broken line), and LT (the purple broken line).

The peak positions of O-H combination on the spectra obtained from (TP+H) (D) and (W) are same.

The absorbance of the amide II disappear on the spectrum of (TP+H) (W).

Fig. 55 Off-line FIR/THz spectra obtained from (TP+H) (D) (the red solid line), (TP+H) (W) (the blue solid line), TP (the orange broken line), and HPC (the light green broken line).

The two characteristic absorptions disappear on the spectrum of (TP+H) (W).

Fig. 56 Off-line FIR/

添付資料6 国内学会発表要旨 2

日本薬剤学会第26年会発表要旨

錠剤コーティング工程解析手法としてのテラヘルツ波技術の導入研究

○坂本知昭¹、中山幸治²、A. Portieri³、D. Arnone³、P. Taday³、笹倉大督⁴、A. Zeitler⁵、川西 徹¹、檜山行雄¹

(¹国立医薬品食品衛生研究所、²東和薬品株式会社、³TeraView Ltd、⁴マルバーンインスツルメンツ、⁵Univ. of Cambridge)

【目的】防湿性や光遮蔽効果などの機能性をもつコーティングは錠剤の品質において重要な役割を果たすため、コーティング工程の解析・評価は品質管理上重要である。演者らはテラヘルツ波技術の製薬評価技術としての導入研究を行っているが、その研究の一環として、時間領域テラヘルツ分光／イメージング技術を用いた錠剤コーティング工程のリアルタイムモニタリング手法の開発を目指した基礎的検討を行っているので、その一部を本年会で報告する。

【実験方法】10w/w%の含量で主薬成分を含むモデルコア錠を作製し、フィルムコーティングを施し、65分まで経時的に錠剤を採取した。各経時点における錠剤(n=6)を Coating Scan TPI imaga 2000 system (TeraView Limited, Cambridge, UK)により測定し、コーティング層におけるテラヘルツ波反射強度の分布及び層厚みの分布のイメージを比較した。

【結果・考察】各錠剤から得られたテラヘルツ電場記録から、コーティング開始後40分、約35μmの厚さからコーティング層の検出が可能であることが分かった。また、層厚の分布では、イメージ作成時に用いるコントラストの影響で、コーティングが検出可能となるまで正確な厚みの分布が示されない可能性が示されたが、反射強度の分布ではリーズナブルな経時的な変化が観察された。年会では他の物性試験の結果も併せてコーティングの機能性評価法としてのテラヘルツ波技術の有用性を報告する。

添付資料7 国内学会発表資料2

日本薬剤学会第26年会発表資料

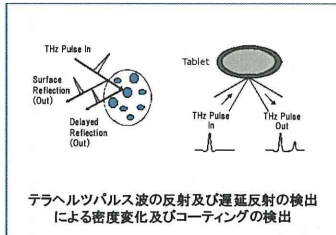
UNIVERSITY OF
CAMBRIDGE

錠剤コーティング工程解析手法としてのテラヘルツ波技術の導入研究

○坂本知昭¹、中山幸治²、A. Portieri³、D. Arnone³、P. Taday³、笠倉大督⁴、A. Zeitler⁵、川西 徹¹、檜山行雄¹
(¹国立医薬品食品衛生研究所、²東和薬品株式会社、³TeraView Ltd、⁴マルバーンインスツルメンツ、⁵Univ. of Cambridge)

緒言

防湿性や光遮蔽効果などの機能性をもつコーティングは錠剤の品質において重要な役割を果たすため、コーティング工程の解析・評価は品質管理上重要である。演者らはテラヘルツ波技術の製薬評価技術としての導入研究を行っているが、その研究の一環として、時間領域テラヘルツ分光/イメージング技術を用いた錠剤コーティング工程のリアルタイムモニタリング手法の開発を目指した基礎的検討を行っているので、その一部を本年会で報告する。



テラヘルツパルス波の反射及び遅延反射の検出による密度変化及びコーティングの検出



コーティング開始後0分(コア錠)、10分、20分、30分、40分、50分、60分、65分(終末点)における錠剤の採取。

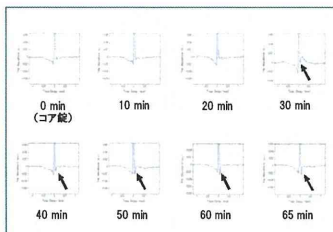


図1 電場記録の経時変化

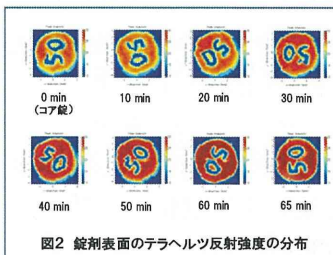


図2 錠剤表面のテラヘルツ反射強度の分布

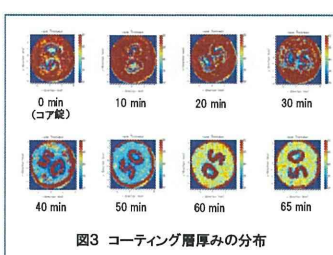


図3 コーティング層厚みの分布

結論

- ▶コーティング開始後30分で、刻印の周囲にコーティング層の形成が観察された。
- ▶電場記録からは、コーティング開始後30分からコーティングの形成を示す負のピークが検出され、コーティングの経時的コーティング層表面における反射波の強度の分布のイメージは経時的に増大した。
- ▶コーティング層の分布イメージでは、コーティングの検出以降、イメージの強度は経時的に増大した。
- ▶イメージ作成時のコントラストの設定でコーティング厚みに変換後の相対値が高く表示されることがあった。
- ▶コーティング層の経時変化では、開始後60分以降はほぼ厚みは一定となり、コーティング工程終了時点の65分はほぼ適切に設定されているものと考えられた。

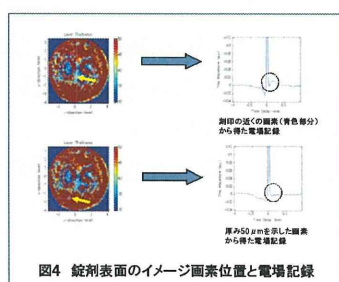


図4 錠剤表面のイメージ画素位置と電場記録

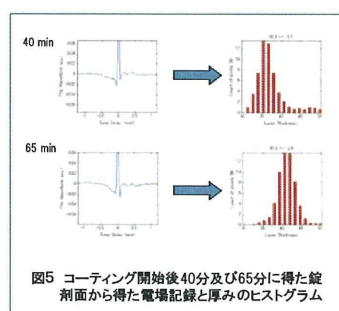


図5 コーティング開始後40分及び65分に得た錠剤面から得た電場記録と厚みのヒストグラム

TeraView

日本薬剤学会第26年会、平成23年5月29日-31日、タワーホール船橋

Malvern

添付資料8 国内学会発表資料3

テラヘルツテクノロジーフォーラム ビジネスセミナー講演資料

テラテクビジネスセミナー 平成24年1月20日



医薬品品質評価科学への遠赤外／テラヘルツ分光法
及びイメージング技術の導入と将来への課題

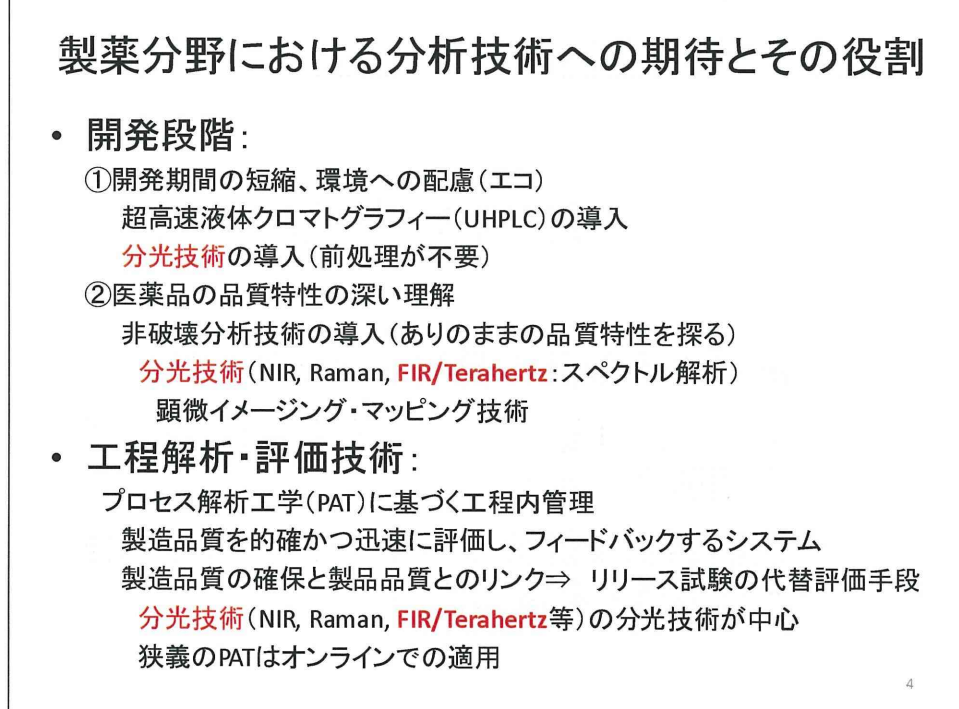
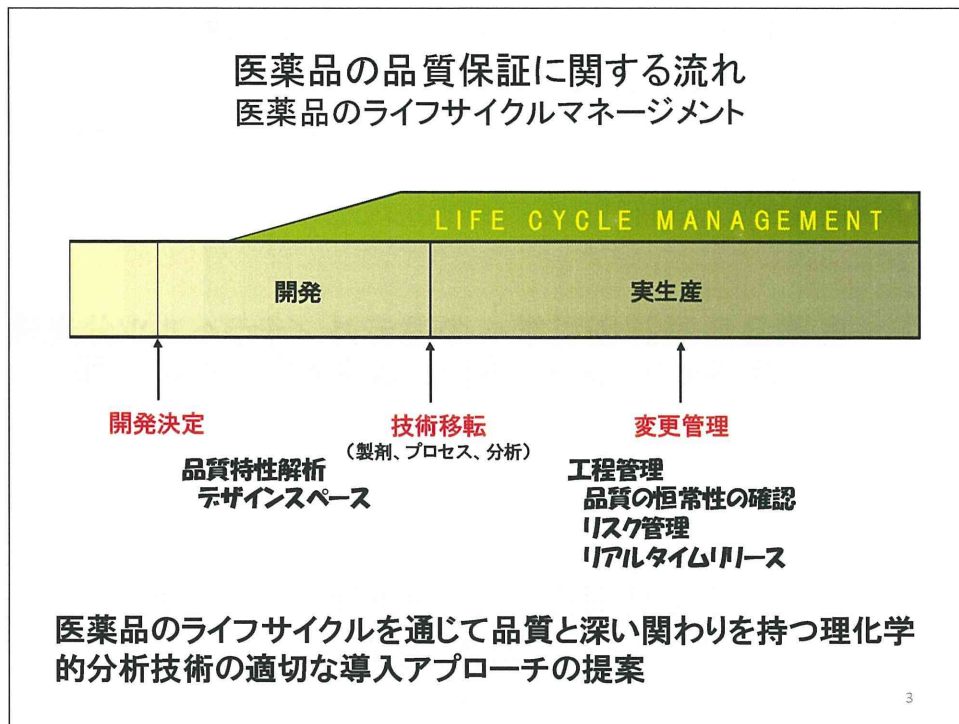
国立医薬品食品衛生研究所 薬品部
坂本 知昭

1

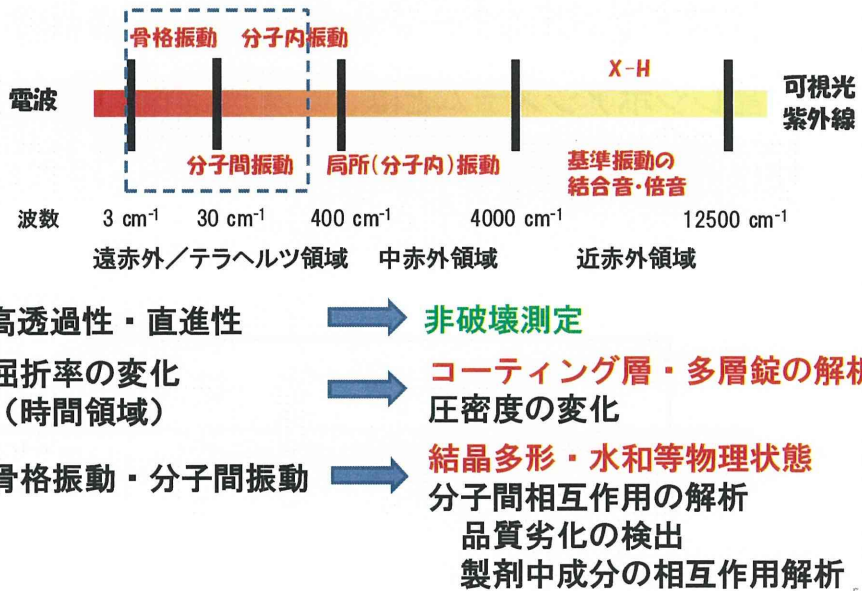
講演の内容

- 最近の医薬品の品質保証と分析技術
- 製薬における遠赤外／テラヘルツ分光の応用研究の紹介
- 医薬品品質評価ツールとしての導入に向けた期待と今後の課題

2



テラヘルツ帯電磁波の製薬分野への技術応用

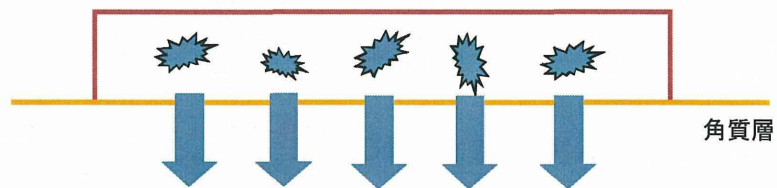


製薬分野における遠赤外／テラヘルツ分光の応用研究の紹介

1. THzパルスイメージング技術を用いた結晶レジボア型TDDSテープ中の主薬結晶の解析
2. コーティング錠の品質特性解析へのTHzパルス分光イメージングの適用
3. コーティング工程におけるテラヘルツ時間領域分光イメージングの導入研究

1. THzパルスイメージング技術を用いた結晶レジボア型TDDS中の主薬結晶の解析

結晶レジボアシステムとは、皮膚透過性の高い主薬成分を基剤中で結晶化させ、基剤からの主薬の放出速度を制御して一定の血中濃度を維持するドラッグデリバリーシステムのこと。



7

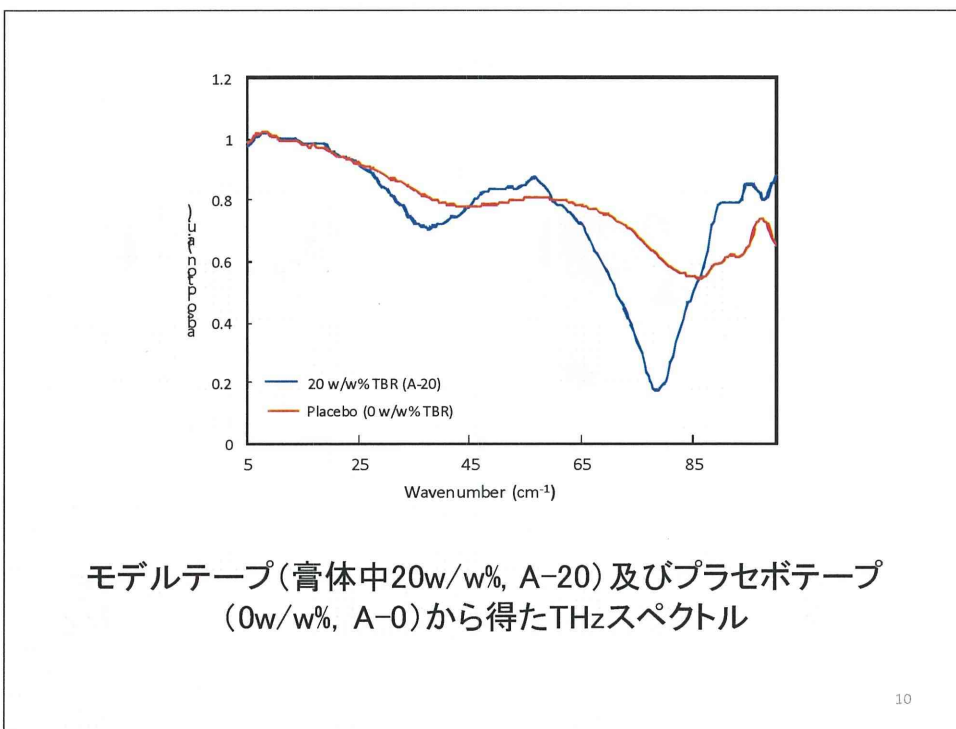
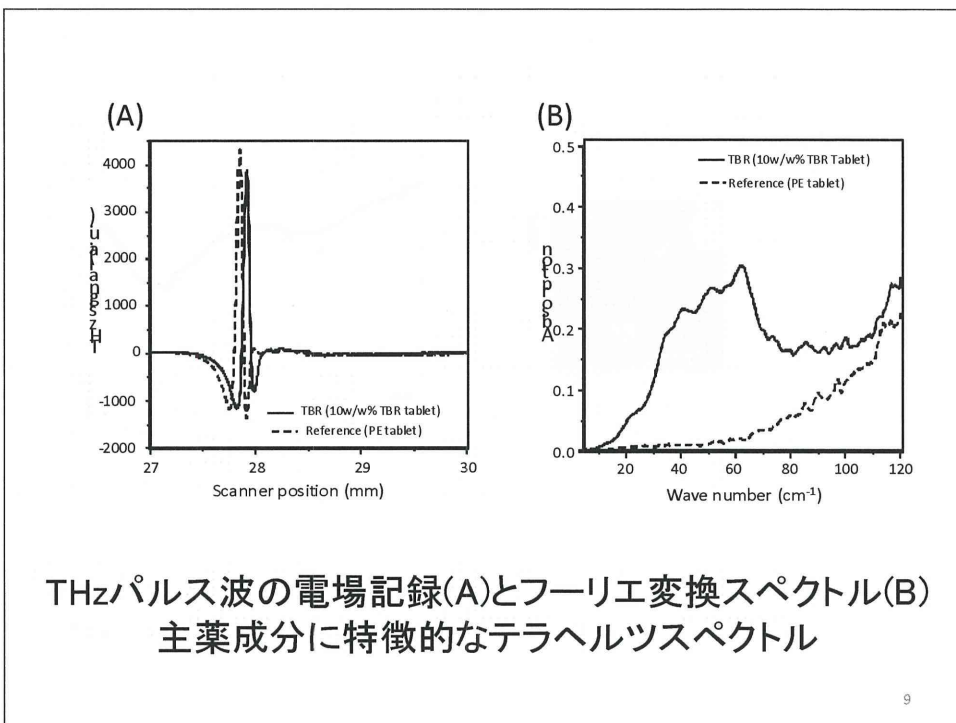
結晶形成の確認

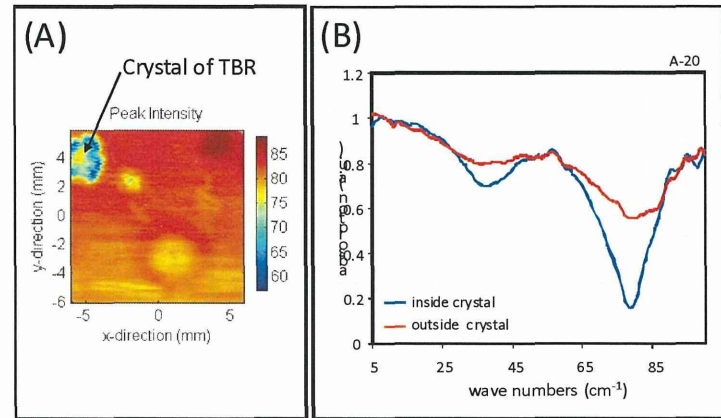
本製剤のように特殊な処方設計がなされている医薬品は、実製造段階以降、その品質特性（処方設計通りに結晶が形成していること）を確認することが難しい。

非破壊で基剤内部の結晶を検出する分析法

結晶生成工程管理等、品質管理への応用

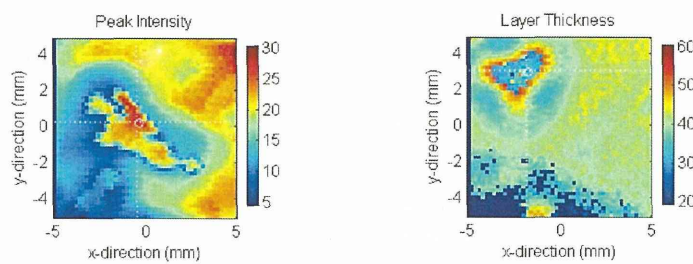
8





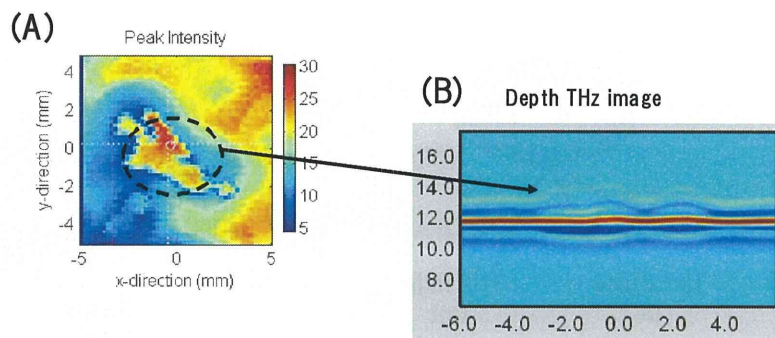
モデルテープ基剤のTHzイメージ(A)と結晶塊内側及び外側に存在する画素から得たTHzスペクトル(B)

11



モデルテープ(30w/w%, A-30)から得たTHzイメージ
(結晶の長径: 0.5mm ~ 3 mm, 結晶の短径: 0.1mm ~ 0.2mm)

12



TBR結晶塊のTHzイメージ(A)と基剤の深さ方向(B-Scan)のTHzイメージ(B)

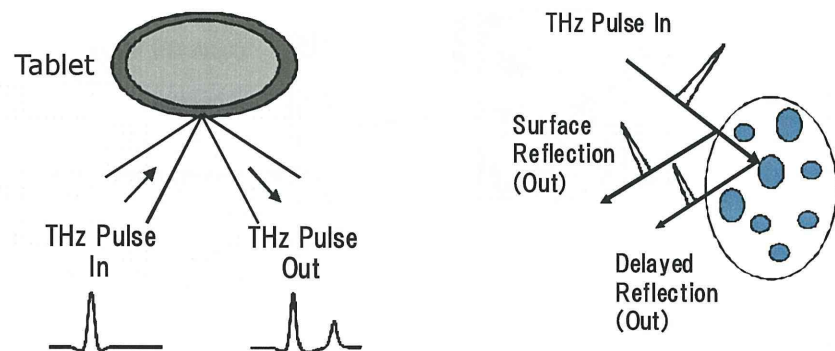
13

2. コーティング錠の品質特性解析へのTHzパルス分光イメージングの適用

- コーティング特性の解析・評価
- 内部圧密度の分布の検出
- 市場流通医薬品の品質確保(確認)
偽造(模造)医薬品対策

14

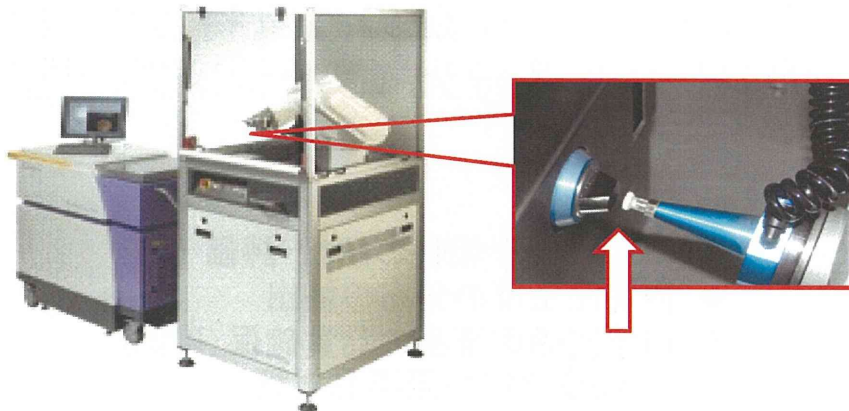
THzパルス波技術を用いた製剤品質特性解析



コーティング層並びに内部異物(密度の変化)に起因するエコー・反射

15

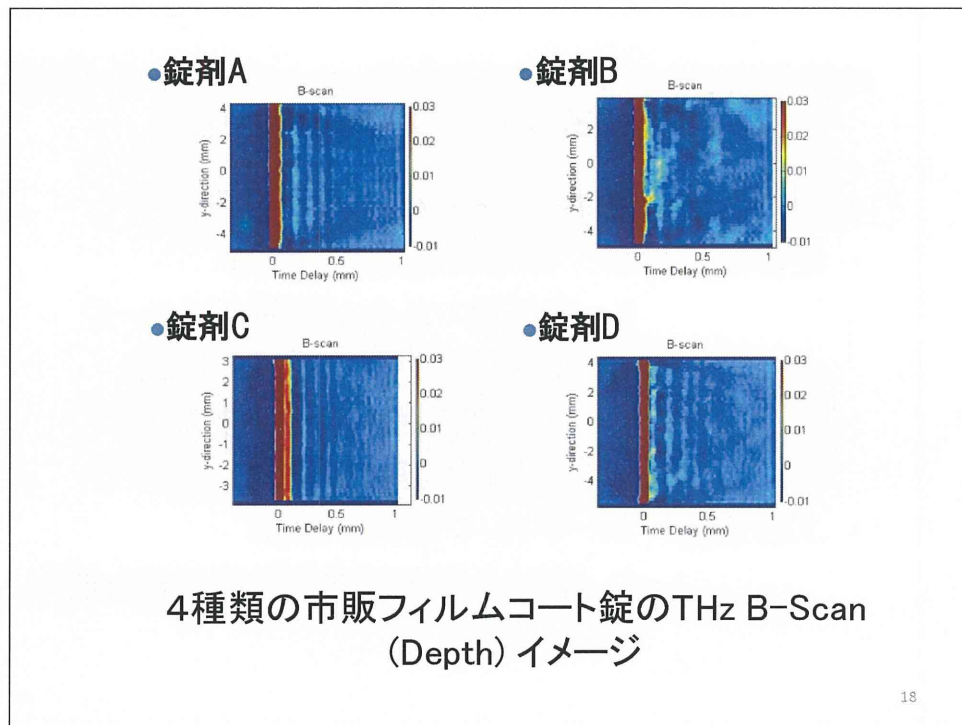
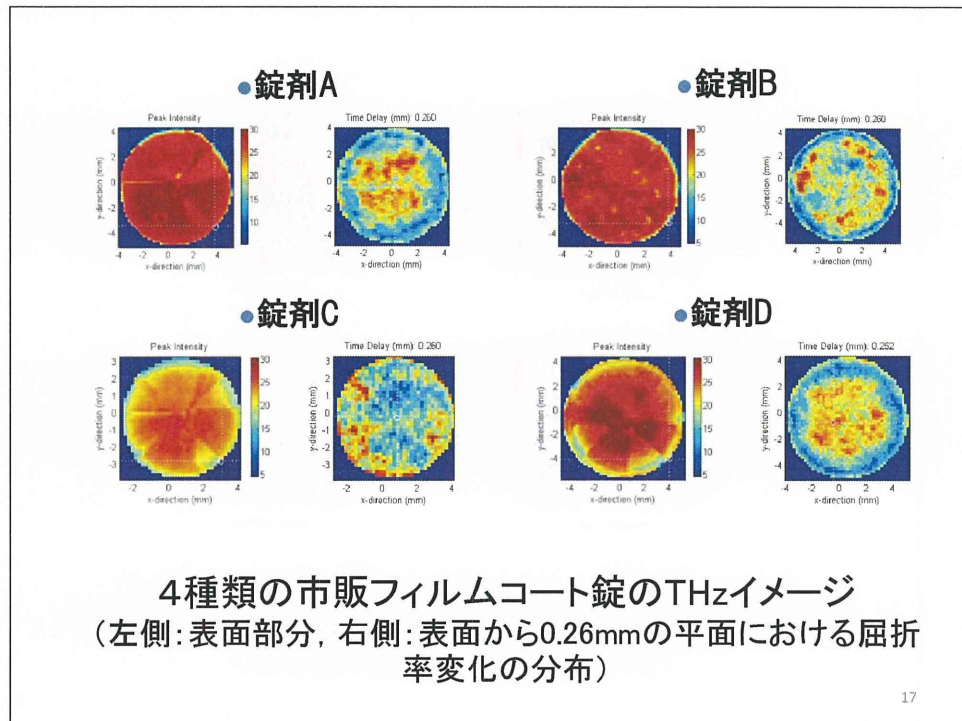
測定装置

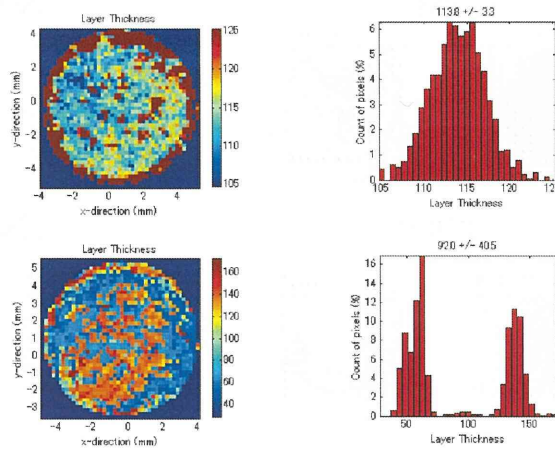


TPI Imega 2000 Coating Scan
TeraView Ltd (Cambridge, UK)

テラヘルツ波照射部及び
検出部

16





コーティング厚の分布イメージと分布のヒストグラム
(上側: 錠剤A, 下側: 錠剤D)

19

時間領域テラヘルツ波技術を用いたコーティング・錠剤内部圧密度分布の解析の有用性

- 製剤開発におけるコーティング層の状態
- 圧密度の分布: 錠剤製造工程を反映
 - ? 同工程であれば同様のイメージ
 - ⇒ 工程の予期せぬ変化の検出
 - ⇒ 市場流通医薬品の品質確保
(偽造医薬品の検出)
- 工程管理: コーティング品質の評価
 - ? 設計品質と同等の製造品質を達成

20

3. コーティング工程におけるテラヘルツ時間領域分光イメージングの導入研究

- コーティングは外観改善、苦味マスクのほか遮光、腸溶性など、機能を期待して施されることが多い
 - 工程管理は通例、コーティング液の噴霧量と乾燥後の質量で確認
- ⇒ コーティングの状態、層の厚みなど直接的に管理できないか？

21

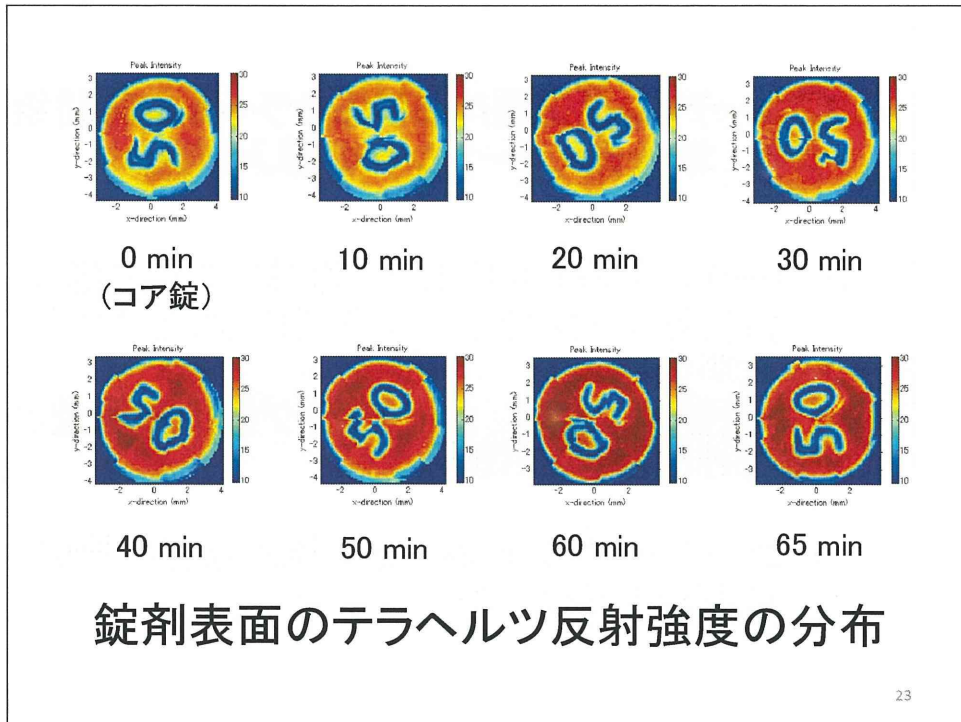
モデルコーティング実験



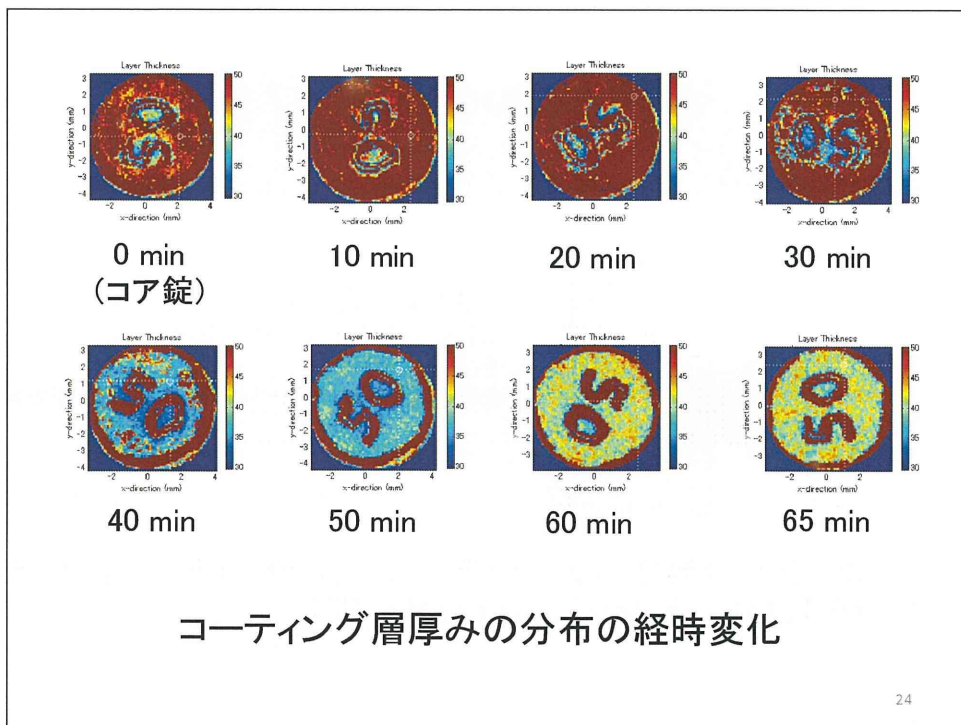
主薬含量 10 w/w%
賦形剤(乳糖一水和物) 約50w/w%
その他 約40 w/w%
の実製剤を模したモデル錠剤(コア錠)を作製

コーティング開始後0分(コア錠)、10分、20分、30分、40分、50分、60分、65分(終末点)における錠剤を採取。

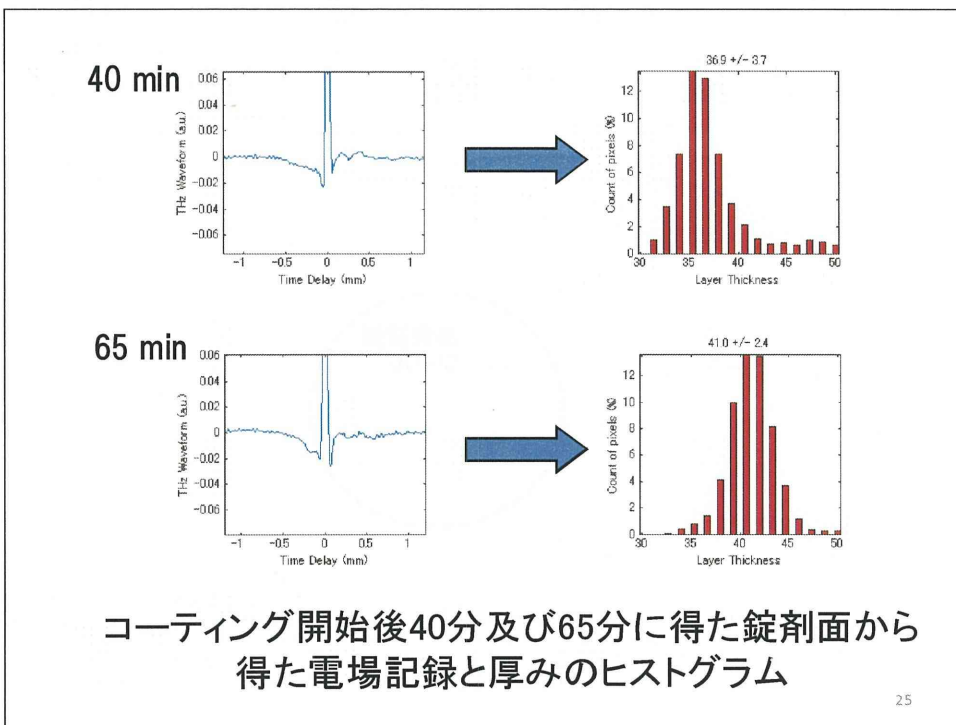
22



23



24

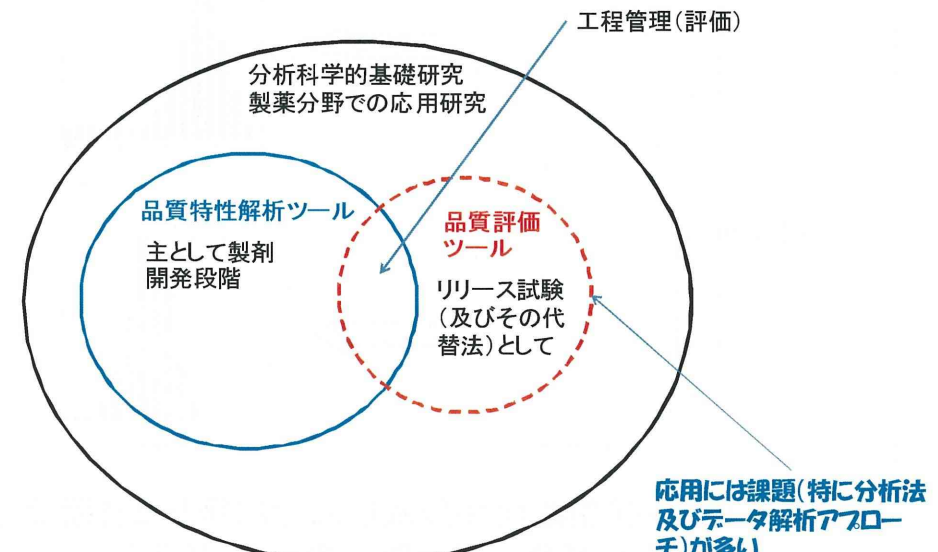


結論

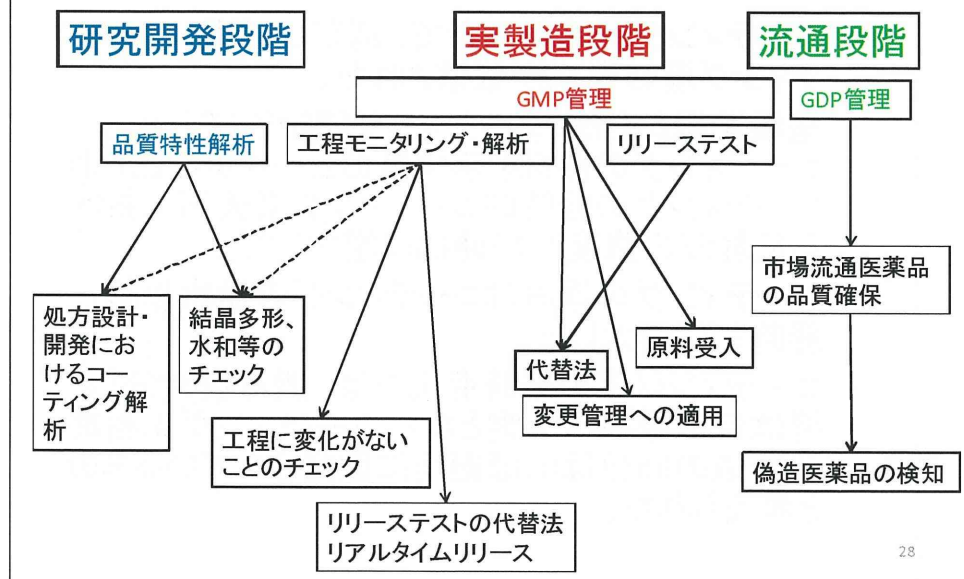
- コーティング開始後30分で、刻印の周囲にコーティング層の形成が観察された。
- 電場記録からは、コーティング開始後30分からコーティングの形成を示す負のピークが検出され、コーティングの経時的コーティング層表面における反射波の強度は経時に増大した。
- コーティングの厚みはコーティングの検出以降、経時に増大した。
- コーティング厚の経時変化では、開始後60分以降はほぼ厚みは一定となり、コーティング工程終了時点の65分はほぼ適切に設定されているものと考えられた。

26

製薬分野での分析技術のポテンシャルと応用



各ステージにおけるFIR/THz分光法への期待 ---導入の一例---



遠赤外／テラヘルツ波技術への期待と 今後の課題



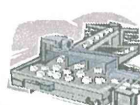
品質特性解析ツール

結晶多形
水和物の識別
コーティング等層の解析
化学結合・相互作用等解析



品質評価ツール

定性・定量分析(リリーステスト)
工程内管理(品質評価)



- 既存の分光分析技術では検知できなかつた分光(物理・化学)情報の獲得
- 他分析法との比較の必要がある場合あり
- 規格・基準の設定に向けた適用の場合には分光学的なバックグラウンドを示す必要あり?

スペクトルの解釈の重要性

29

ご清聴ありがとうございました

30